CERTIFICATE OF MAILING
37 C.F.R. §1.8

I hereby certify that this correspondence is being deposited with the U.S. Postal Service with sufficient postage as First Class Mail in an envelope addressed to: Box PCT, Assistant Commissioner for Patents, Washington, DC 20231, on the date below:

May 22, 2001
Date

Steven L. Highlander

PATENT

IN THE UNITED STATES PATENT AND TRADEMARK OFFICE

In re Application of:
Theodore W. RANDOLPH *et al.*

Serial No.: 09/350,327

Filed: July 9, 1999

For: HIGH PRESSURE REFOLDING OF PROTEIN AGGREGATES AND INCLUSION BODIES

Group Art Unit: 1651

Examiner: H. Guttman

Atty. Dkt. No.: UTEC:003/SLH

Considered
July 26, 2001

DECLARATION OF THEODORE W. RANDOLPH

Commissioner for Patents
Washington, D.C. 20231

I, Theodore W. Randolph:

1. I am the Theodore W. Randolph listed as an inventor on the above-captioned application. I currently hold the position of Professor in the Department of Chemical Engineering at the University of Colorado (Boulder).

2. I understand that the examiner in charge of the above-captioned application has questioned the enablement of the present claims. In particular, I understand that the examiner has raised

questions regarding the enablement of two-step pressurization methods, and the broad application of the claimed methods to proteins in general. In response, I would like to provide the following information for the examiner's consideration.

Materials and Methods

3. Purified recombinant DNA derived rhIFN-γ in 5 mM sodium succinate, pH 5.0 (succinate buffer) was provided by Genentech Inc., stored at 4°C until use and used without further purification. This protein is a dimer in its native state. 40 mM pyridine acetate, pH 5.0 buffer (PyrAc buffer) was used for gas-phase electrophoretic mobility mass analysis (GEMMA). Succinate buffer was used in all other experiments. Protein standards (bovine serum albumin, glucose oxidase, hemoglobin, ubiquitin and thyroglobulin) were purchased from Sigma. All chemicals were of reagent grade or higher and were purchased from Sigma as well.

4. Aggregates were prepared by inducing aggregation either by raising the solution temperature to 40°C or by adding guanidine hydrochloride to the protein solution such that the final guanidine hydrochloride concentration was 0.45 M. The extent of the aggregation reactions were in excess of 95% in all cases. The extent of reactions was determined from the well-characterized aggregation rates both for the thermally-induced aggregation, which is second-order in protein concentration and for the guanidine hydrochloride-induced aggregation reaction, which is first-order in protein concentration. Guanidine hydrochloride-induced aggregates were washed with sufficient fresh buffer so that the final guanidine hydrochloride solution concentration was below 5 mM.

Aggregates for refolding experiments were suspended in fresh buffer at approximate concentrations of 1, 10 and 20 mg/mL rhIFN-γ.

5. The high-pressure equipment used for refolding experiments consisted of a high-pressure reactor, high-pressure UV spectroscopy cell, metallic gauge (accurate to +/- 2 MPa) and generator. The high-pressure reactor and high-pressure UV spectroscopy cell were designed and fabricated in our laboratory. The gauge and generator were purchased from High Pressure Equipment, Co, (Erie, PA). For any given experiment, either the high-pressure reactor or high-pressure UV spectroscopy cell was employed.

6. The high-pressure UV spectroscopy cell was made of 316 stainless steel, sealed with Buna-N 90 durometer o-rings and had an optical port diameter of 6 mm and pathlength of 7.65 mm. The cell utilized cylindrical sapphire windows (16 mm diameter, 5.1 mm thick) and was capable of experiments up to 250 MPa. Separation of the sample from the pressure transmitting fluid (silicon oil) was facilitated by a piston device external to the cell. All wetted metal surfaces were constructed of 316 SS. All *in situ* high-pressure UV experiments were conducted at a protein concentration of *ca.* 1 mg/mL.

7. For experiments conducted in the high-pressure reactor, aggregate suspensions were loaded into *ca.* 1 mL polypropylene bulbs, heat-sealed and loaded into the reactor. The reactor was sealed and the pressure increased to 250 MPa, which is sufficient pressure to ensure that, at equilibrium, rhIFN-γ is fully dissociated into monomers. The samples were held at 250 MPa for sufficient time to dissolve the aggregates and for the protein

equilibrate, based upon *in situ* second-derivative UV measurements (see below). The pressure was then lowered to 100 MPa and again held for sufficient time to reach equilibrium for rhIFN-γ concentrations of *ca.* 1 mg/mL (see below), after which the pressure was reduced to 0.1 MPa and the samples were removed from the high-pressure reactor.

8. TEM was performed on samples of native, aggregated and pressure-treated aggregates rhIFN-γ that had been negatively stained with a 2% solution of uranyl acetate at total a protein concentration of *ca.* 1 mg/mL. Specimens were stained on formvar/carbon 400 mesh copper grid and were viewed on a JOEL 100CX TEM with an accelerating voltage of 80,000 kV. Micrographs of aggregate structures were obtained at magnifications from 20,000 to 80,000.

9. The procedure for GEMMA particle size analysis has been previously described and was based on the method of Kaufman *et al.*, *Anal. Chem.* 68(11):1895-1904 (1996). The instrument was calibrated using protein standards of known molecular weight (MW). A linear calibration curve was developed from the natural log of the electrophoretic mobility (EM) diameters versus the natural log of MW. Samples of native, aggregated and pressure-treated aggregates of rhIFN-γ were diluted to *ca.* 1 to 2 μg/mL into PyrAc buffer, which has a conductivity of *ca.* 2 $m\Omega^{-1}$ cm, and immediately analyzed using a GEMMA analyzer from TSI (St. Paul, MN). PyrAc buffer was employed due to the GEMMA requirement of less than 1 ppm non-volatile material in the sample.

10. The GEMMA analyzer consisted of a model 3480 electrospray aerosol generator, a model 3085 differential mobility analyzer (DMA), a model 3025A ultrafine condensation particle counter (CPC). Dried and filtered air was delivered at a rate of 1 Lpm from the utility air supply through a model 307402 filter/dryer and instrument-grade carbon dioxide was delivered at a rate of 0.05 to 0.1 Lpm. The fused-silica electrospray capillary was 25 cm long and had an internal diameter of 25 μm. Sample flow (*ca.* 100 nL/min) was facilitated by a differential pressure of 25 kPa (3.7 psi) across the capillary. An electrical potential of 2 kV was maintained across the capillary, with a corresponding current of 200 to 250 nA.

11. Data acquisition was made via Aerosol Instrument Manager (AIM®) version β 4.10 software from TSI on an IBM compatible PC running Microsoft Windows 95®. The data acquisition software used 64 log-spaced channels per decade of EM diameter. Sample analysis was made from *ca.* 2.5 to 58 nm and acquisition times from 3 to 6 minutes, using assumed values for air viscosity (μ) of 1.82 x 10^{-5} kg/(m s), mean free path (λ) of 7.75 x 10^{-8} m and protein density (ρ) of 1.2 g/mL. Data files, in units of mass percent concentration, were exported as text files and imported into Microsoft Excel®. EM diameters were determined by the maximum of a given peak. Monomer to dimer ratios and extent of reactions (based on mass percent dimer) were determined by finite integration of the individual peaks in the mass percent distributions.

12. Dynamic light scattering measurements were performed on the thermally-induced aggregates of rhIFN-γ using a Nicomp 370 Submicron Particle Sizer (Particle Sizing Systems, Santa Barbara, CA). The total protein concentration was 1 mg/mL.

13. Absorption spectra were measured with a Perkin-Elmer Lambda 3B dual-beam spectrophotometer at rhIFN-γ concentrations of *ca.* 1 mg/mL. Scans were measured from 310 nm to 250 nm with scan rate of 15 nm per minute. Data acquisition was made via a National Instruments (Austin, TX) model AT-MIO-16E-10 data acquisition board at a rate of 5 samples per second. National Instruments LabView® software was used to control data acquisition and Microsoft Excel® to convert the wavelength and absorption data from volts to nm and absorbance units, respectively. The second derivatives of the absorption spectra ($d^2A/d\lambda^2$) were calculated in Grams/386 (v. 3.02) software (Galactic Industries) using the Savitzky-Golay method with a second order polynomial smoothed over +/- 2 nm.

14. Temperature was controlled using recirculating fluid thermostated by a Lauda model M3 recirculating bath temperature controller. Spectra for samples treated in the high-pressure reactor were collected at atmospheric pressure with the samples in standard 10 mm pathlength quartz cuvettes and the appropriate blank placed in the reference cell of the spectrophotometer. For experiments carried out in the high-pressure cell, absorption spectra were collected for the sample and buffer separately, with no reference sample in the spectrophotometer. Subtraction of the buffer spectrum, collected at the appropriate

pressure, from the protein spectrum was carried out in Grams/386® (v. 3.02) software prior to calculation of the second derivative.

15. IR spectra were collected using an adjustable pathlength cell set at 8 μm. Blank buffer spectra were collected using the same cell under an identical solution condition, with no protein present. All spectra were collected at atmospheric pressure on a Nicolet Magna-IR® 750 series II (Madison, WI) spectrometer equipped with a DTGS detector. Interferograms were collected in the single beam mode, signal-averaged over 256 (for samples at *ca.* 20 mg/mL) and 1024 (for samples at *ca.* 10 mg/mL) scans at a resolution of 4 cm^{-1} using Omnic® (v. 2.1) Software from Nicolet. The optical bench and sample chamber were continuously purged with dry air supplied from a Whatman model 75-52 FTIR purge gas generator (Haverhill, MA). Single beam spectra of both protein-in-buffer and buffer were reprocessed into absorbance spectra by subtracting out the background spectra from each. Nicolet software was used to subtract the buffer and water vapor contributions from the protein-in-buffer spectra and to calculate the second derivative. The remaining spectrum was 7-point smoothed to remove white noise and imported into Grams/386® (v. 3.02) software (Galactic Industries) where it was baseline corrected and area normalized per method of Dong *et al.*, *J. Pharm. Sci.* 84(4):415-424 (1995).

16. The presence of soluble aggregates and monomer/dimer content of pressure-treated aggregates was measured by SEC and compared to the liquid control. Insoluble aggregates were removed by centrifugation and the supernatant was assayed by size exclusion chromatography (SEC). 50 μL aliquots of the supernatant, diluted to 1 mg/mL

in succinate buffer, were loaded onto a silica-based Tosohaas TSK-GEL G2000SW$_{XL}$ column. The mobile phase, 1.2 M KCl, was pumped at a rate of 0.8 mL/min and absorbance at 214 nm was monitored as a function of time. Resultant chromatograms were imported into Grams/386® (v. 3.02) software where they were area normalized and curve fit to determine the percent contributions and elution times for the monomer and dimer. The Autofind curve fit function was employed with parameters set for a maximum of two peaks, Guassian curve, medium sensitivity and offset baseline. The instrument was calibrated using protein standards of known MW. A linear calibration curve was developed from the natural log of the elution time versus the natural log of MW.

Results

17. At protein concentrations above 5 mg/mL, thermally-induced aggregates of rhIFN-γ formed a colorless, transparent gel with high viscosity that could not be concentrated by centrifugation. At concentrations of *ca.* 1 mg/mL, the protein concentration was sufficiently low that the viscosity increase upon aggregation was minimal and separation by centrifugation was possible. Like the aggregates formed at higher protein concentrations, the aggregates formed at concentrations of *ca.* 1 mg/mL were colorless and scattered relatively little light. In contrast to aggregates formed by high temperatures, the addition of guanidine hydrochloride to solutions of rhIFN-γ resulted in the formation of a white, opaque precipitate that was easily centrifuged from solution, regardless of the aggregation protein concentration.

18. Electron micrographs of the aggregates revealed that the thermally-induced aggregates formed a matrix of fiber-like strands of indeterminate length (Figure 1A), but the guanidine hydrochloride-induced aggregates formed an amorphous precipitate (Figure 1B). The thermally-induced aggregate fibrils have a consistent diameter on the order of 10 nm. No amorphous structures were observed in the thermally-induced aggregates. Conversely, no fibrous structures were found in the guanidine hydrochloride-induced aggregate samples.

19. The electrophoretic mobility diameter distribution of native rhIFN-γ and thermally induced aggregates was measured by GEMMA and the results are presented in Figure 2. The native protein, equilibrated at 25°C and 1 mg/mL in PyrAc buffer, was found to have two significant peaks centered at 4.4 and 5.5 nm (Figure 2A). The peaks corresponded to particles having molecular weights of 16 and 32 kD, respectively, based on the calibration curve with known protein standards. These molecular weights are in good agreement with the known molecular weights for the monomer and dimer of rhIFN-γ (16.45 and 32.9 kD, respectively). No other significant peaks were detected in the native sample if the concentration of the sample was kept below *ca.* 3 μg/mL. The mass percent monomer detected by GEMMA (*ca.* 12% in Figure 2A) has been determined to be artificially high from dissociation equilibrium experiments. The bias towards the monomer is caused by surface-induced dissociation of the native dimer on the electrophoresis capillary. The thermally-induced aggregate sample, aggregated at 40°C and 21 mg/mL for 48 hours in succinate buffer, had *ca.* 1 and 4% by mass of monomer

and dimer, respectively. The aggregates (Figure 2B), in excess of 95% by mass, had a mass average diameter of 16.5 nm, corresponding to an average effective MW of 980 kD based on the calibration curve with known protein standards.

20. The region between 275 and 295 nm of the second derivative UV spectrum reflects the microenvironments of tryptophan and tyrosine residues and is affected by the conformational state of proteins (Balestrieri *et al.*, *Euro. J. Biochem.*, 90(3):433-44 (1978); Ragone *et al.*, *Biochem.* 23(8):1871-1875 (1978); Servillo *et al.*, *Anal. Biochem.*, 126(2):251-257 (1982). Since the derivative UV spectra of tyrosine and tryptophan are minimally affected by pressure (Lange *et al.*, *Euro. Biophys. J. Biophys. Lett.*, 24(5):277-283 (1996), changes to the second derivative UV spectrum of rhIFN-γ by pressure result from changes to the native conformation (Webb *et al. Biotechnol. Prog. 16(4):630-36* 2000). The second derivative UV spectra of native, pressure dissociated soluble protein and thermally-induced and guanidine hydrochloride-induced aggregate forms of rhIFN-γ in 5 mM sodium succinate buffer are presented in Figure 3. The wavelength position of the extremum located near 286 nm for native and dissociated forms of rhIFN-γ is independent of the degree of dissociation and its relative height has been shown to indicate the degree of dissociation of rhIFN-γ. Thus, the relative height of this extremum can also be used to follow the extent of reassociation and refolding of rhIFN-γ in the absence of aggregates.

21. The spectra of the two aggregate forms (thermal- and guanidine hydrochloride-induced) show similar deviations from the native second derivative UV spectrum and are distinct

from the both the native and pressure-dissociated spectra (Figure 3). The aggregate spectra display an overall dampening of the signal amplitude and a blue-shift in the absorbance spectra, both of which indicate increased exposure to hydrophilic environments of the tryptophan and tyrosine residues relative to the native structure (Lange *et al.*, *Euro. Biophys. J. Biophys. Lett.*, 24(5):277-283 (1996); March & Middaugh, *Anal. Biochem.*, 222(2):323-331 (1994)). Additionally, both aggregate spectra show significant reduction in the depth of the minimum located near 280 nm. However, there are notable differences between the aggregate second derivative UV spectra. The extent of perturbation from the native spectrum, as measured by amplitude reduction and wavelength shift, is less severe with the thermally-induced aggregate spectrum compared with the guanidine hydrochloride-induced aggregate spectrum. Further, there is significant band broadening in the maxima located near 288 and 280 nm for the guanidine hydrochloride-induced aggregate spectrum that is not apparent in the thermally-induced aggregate spectrum.

22. To compare the secondary structures of the two aggregates with each other as well as the native form, FTIR absorbance spectra of all three states were collected and second derivative spectra calculated and compared. Figure 4 is a plot of the second derivative FTIR spectra of native rhIFN-γ in buffer and both the thermal- and guanidine hydrochloride-induced aggregates of rhIFN-γ. Significant perturbations from the native state are observed in both aggregate forms, with a wavelength shift of and a loss of absorbance in the α-helix band (near 1656 cm^{-1} in the native spectrum) and concomitant appearance of intermolecular β-sheet bands near 1620 and 1695 cm^{-1} (Figure 4). The

contributions of the intermolecular β-sheet bands near 1620 and 1695 cm^{-1} are comparable for both aggregate forms, as is the extent of loss in α-helix. Only minor differences in β-sheet (region near 1630 to 1645 cm^{-1}) and turn structures (region near 1670 to 1685 cm^{-1}) are apparent between the temperature- and guanidine hydrochloride-induced aggregates.

23. When guanidine hydrochloride-induced aggregates of rhIFN-γ were exposed to 250 MPa, there was rapid and complete loss of light-scattering aggregates, as measured by absorbance at 310 nm (Figure 5A). The total rhIFN-γ concentration was 1 mg/mL and the guanidine hydrochloride concentration in solution was *ca.* 5 mM. Once dissolution of the aggregates was complete, absorbance scans were collected at 250 MPa and derivative spectra calculated. The pressure was maintained at 250 MPa until the second derivative spectrum no longer changed with time (*ca.* 30 minutes). The second derivative spectrum of guanidine hydrochloride-induced aggregates at 250 MPa equilibrated to the spectrum obtained when native rhIFN-γ is dissociated with pressure at 250 MPa (Figure 3), indicating complete disruption of the aggregate structure and dissociation of the dimeric structure to monomer.

24. Once the second derivative spectrum displayed no further changes with time at 250 MPa, the pressure was reduced to 100 MPa and absorbance spectra collected over time. The second derivative spectra were again calculated and compared until changes with time were no longer observed. At 100 MPa, the extremum near 286 nm (a maximum in the pressure dissociated spectrum, see Figure 3) decreased in height with time and eventually

became a minimum as the protein began to assume a more native conformation. Figure 5B is a plot of the height of the extremum near 286 nm versus time at 100 MPa for the reassociation/refolding of rhIFN-γ at 1 mg/mL, after the guanidine hydrochloride-induced aggregates were dissociated at 250 MPa. Superimposed on Figure 5B are heights of the spectra for the pressure dissociated and native forms of rhIFN-γ as well for the equilibrium pressure-refolded form (1 mg/mL rhIFN-γ), achieved by lowering the pressure to 0.1 MPa. The refolding at 100 MPa is complete in *ca.* one hour and the 286 nm extremum height of the pressure-treated aggregate has returned nearly completely to that of the native control.

24. The rate of dissolution of thermally-induced aggregates at pressure could not be quantified by absorbance changes at 310 nm with time because the aggregates did not scatter light sufficiently. As well, the dissolution of aggregates at pressure can not be followed in the region between 275 and 295 nm either because aggregate dissolution and structural migration to the pressure-dissociated form (Figure 3) occur simultaneously. Thus, the rate of thermally-induced aggregate dissolution at pressure cannot be directly compared with the pressure dissolution of guanidine hydrochloride-induced aggregates. However, the time required for the thermally-induced aggregate to assume the pressure-dissociated state (*ca.* 2 hours), measured by second derivative UV, is significantly slower compared to the time required for guanidine hydrochloride-induced aggregates (*ca.* 30 minutes) to assume the pressure-dissociated state (data not shown). But once the pressure-dissociated state is achieved, the refolding rates are comparable (Figure 5B).

25. Thermally- and guanidine hydrochloride-induced aggregates of rhIFN-γ in buffer at protein concentrations of *ca*. 1, 10 and 20 mg/mL were pressurized to 250 MPa for five hours. The pressure was then lowered to 100 MPa for one and one-half hours, then again lowered to 0.1 MPa. Analysis of the pressure treated aggregates was made both immediately following and two weeks after pressure treatment to assess the effectiveness of the pressure treatment on acquisition of native-like characteristics from aggregates and the stability of the pressure-treated aggregates against re-aggregation, respectively. TEM, GEMMA and HPLC were employed to physically characterize the pressure-treated aggregates and second derivative UV and FTIR spectroscopies were used to structurally characterize the pressure-treated aggregates. Comparison of the results for each technique was made among the pressure-treated aggregates, the aggregate controls and native liquid rhIFN-γ control.

26. Upon depressurization, all thermally- and guanidine hydrochloride-induced aggregate samples were optically clear with no particulates visible to the eye. Additionally, the 10 and 20 mg/mL thermally-induced aggregate samples, which were gelatinous solids prior to pressure treatment, were liquids with viscosities indistinguishable (judged qualitatively) from the native liquid controls.

27. TEM was performed on the liquid control and on the 1 and 20 mg/mL (pressurized and control) samples for both types of aggregates at a total protein concentration of *ca*. 1 mg/mL (20 mg/mL samples were diluted immediately after pressure treatment). Figure 6 contains representative TEM micrographs of pressure-treated (A) thermally-induced and

(B) guanidine hydrochloride-induced aggregates of rhIFN-γ along with (C) the liquid control. Aggregate controls were unchanged from the structures initially observed and, therefore, micrographs of the aggregate controls are not presented in Figure 6 (see Figure 1 for representative structures of the aggregate controls). All micrographs in Figure 6 are at a magnification of 40,000. In both pressure-treated samples and the liquid control, amorphous and fibrous structures were observed, with amorphous material more prevalent than fibrous. Figure 6 A2 displays an amorphous structure from pressure-treated thermally-induced aggregates, which is representative of the dominant structure found for all three samples of rhIFN-γ. The observed structures and frequency of amorphous material relative to fibrous material in both pressure-treated aggregates and the liquid control were consistent. Additionally, there was no observed difference between the samples that were pressure-treated at 1 or 20 mg/mL for both the thermal- and guanidine hydrochloride-induced aggregates. The fibrous network observed in the thermally-induced aggregate samples prior to pressure treatment was destroyed and a large proportion of the pressure-treated thermally-induced aggregate was amorphous. As well, the fibrous material that was observed in the pressure-treated guanidine hydrochloride-induced sample was not found in the guanidine hydrochloride-induced aggregate controls.

28. The fibrous structures seen for the pressure-treated aggregates and the liquid control were shorter in length and more varied in diameter than the fibrous structures observed in the thermally-induced aggregate controls. The lengths of the fibrous structures in the pressure-treated aggregates and the liquid control were generally 100 to 1000 nm in

length and the diameters were typically *ca.* 12 nm but ranged up to *ca.* 25 nm. Some intertwined networks of fibrils were observed in all three sample sets and examples are given in Figures 6 A3 and C2. It was concluded that the morphologies of the pressure-treated aggregates are indistinct from the control and that TEM sample preparation, which involves drying of the protein sample, induced structures consistent with both amorphous and fibrous aggregates.

29. Following the pressure-treatment, UV and FTIR absorbance spectra were collected and second derivative UV and FTIR spectra calculated for pressurized and control samples. The 10 and 20 mg/mL samples were diluted immediately after depressurization such that all UV analysis was conducted at 1 mg/mL rhIFN-γ. Due to concentration limitations of the technique, FTIR spectroscopy was performed only on the 10 and 20 mg/mL samples.

30. Figure 7 is a plot of the second derivative UV spectra of (A) thermally-induced and (B) guanidine hydrochloride-induced, pressure-treated aggregates. Spectra were recorded at 0.1 MPa after the pressure-treatment protocol. For reference, the second derivative UV spectrum of native rhIFN-γ is superimposed on both windows of Figure 7. The aggregate control spectra are omitted from Figure 7 for clarity (see Figure 3 for spectra of aggregates). The extent of recovery of the native second derivative UV spectrum is aggregate-form independent. But, the degree of recovery of the native second derivative UV spectrum is concentration dependent, with greater recovery of the native spectrum at lower protein concentrations. At 1 mg/mL, the pressure-treated aggregates recover nearly identical second derivative UV spectra as the native rhIFN-γ liquid control. Table

2 contains the summary of the percent recovery of the native spectrum measured by second derivative UV spectroscopy, using the ratio of the difference in heights of the extrema near 286 nm between the refolded and pressure-dissociated state relative to those of the native and pressure-dissociated states.

31. Figure 8 is a plot of the area-normalized second derivative FTIR spectra of pressure-treated (A) thermally-induced and (B) guanidine hydrochloride-induced aggregates of rhIFN-γ for pressure-treatments conducted at 10 and 20 mg/mL. Due to the preparation and sample collection times associated with the FTIR technique, FTIR spectra were collected within three hours of depressurization. For comparative purposes, the second derivative FTIR spectrum of native rhIFN-γ is superimposed on both windows of Figure 8. As was the case with the UV spectroscopic results, the recovery of native secondary structure, measured qualitatively by FTIR, is aggregate-form independent, as the second derivative FTIR spectra at 10 and 20 mg/mL are the same for both aggregate forms, respectively. There is substantial reduction in the intermolecular β-sheet bands near 1620 and 1695 cm^{-1} with pressure treatment for both the 10 and 20 mg/mL samples. But, the reduction of these intermolecular β-sheet bands to levels observed in the native spectrum is nearly complete for the 10 mg/mL spectra, while significant bands are still present near 1620 and 1695 cm^{-1} in each of the 20 mg/mL spectra. As measured by second derivative FTIR, the samples pressure-treated at 10 mg/mL recover all of the α-helix seen in the native structure (band near 1656 cm^{-1}). The recoveries of native secondary structure, as measured by area of overlap (Kendrick *et al.*, *J. Pharm. Sci.*, 85(2):155-158 (1996)), are *ca.* 90 and 70% for the 10 and 20 mg/mL pressure-treatments, respectively.

32. In conclusion, I submit that the foregoing data provide evidence on two major issues raised by the examiner. First, the data show that a two-step depressurization method does, in fact, provide a working refolding process. Second, the ability to refold a dimeric protein demonstrates that even complex proteins are amenable to refolding using methods according to the present invention.

33. I hereby declare that all statements made of my own knowledge are true and all statements made on information are believed to be true and further that the statements were made with the knowledge that willful false statements and the like so made are punishable by fine or imprisonment or both under § 1001 of Title 18 of the United States Code, and that such willful false statements may jeopardize the validity of this application or any patent issued thereon.

April 26, 2001

Date

Dr. Theodore W. Randolph

LEGENDS TO FIGURES IN DECLARATION

Figure 1: TEM micrographs of rhIFN-γ (A) thermally-induced aggregates and (B) guanidine hydrochloride-induced aggregates. Frames A1 and B are at a magnification of 40,000 (Bar = 200 μm) and A2 at 80,000 (Bar = 100 μm).

Figure 2: Mass percent concentration versus EM diameter as measured by GEMMA for native (thick line) and thermally-induced aggregates (thin line) of rhIFN-γ. (A) EM diameter region for monomer (*ca.* 4.4 nm) and dimer (*ca.* 5.5 nm) and (B) EM diameter region for aggregates. Note that the particle size distribution is split into two windows for clarity and that the two windows have different mass percent scales. The response for native rhIFN-γ in the 7 to 10 nm range (window B) is within the noise level of the instrument.

Figure 3: Second derivative UV spectra of rhIFN-γ thermally-induced (□) and guanidine hydrochloride-induced (▲) aggregates prior to pressure treatment. Included with the spectra of aggregates are rhIFN-γ liquid control at 0.1 MPa (solid line) and pressure-dissociated at 250 (X) MPa. The extremum near 286 nm in the native and pressure-dissociated spectra was used to follow the refolding event after dissociation of aggregates. Except for the 250 MPa spectrum, all spectra were collected at 0.1 MPa.

Figure 4: Area normalized second derivative FTIR spectra of thermally-induced aggregates (□) and guanidine hydrochloride-induced aggregates (▲) prior to pressure treatment. The spectrum of native rhIFN-γ is included for comparative purposes and is represented as a solid line. All spectra were collected at 0.1 MPa.

Figure 5: (A) Absorbance at 310 nm versus time for guanidine hydrochloride-induced aggregates at 250 MPa in succinate buffer. The total rhIFN-γ concentration was 1.0 mg/mL and the guanidine hydrochloride concentration in solution was *ca.* 5 mM. The absorbance of native rhIFN-γ at 310 nm in the absence of aggregates is *ca.* 0.06 AU mL/cm mg (data not shown). (B) The second derivative extremum (near 286 nm) height versus time at 100 MPa for rhIFN-γ (1

mg/mL) guanidine hydrochloride-induced (▲) and thermally-induced (□) aggregates dissociated at 250 MPa. Error bars of are 95% confidence intervals on the spectral height. Spectral heights for the pressure-dissociated form at 250 MPa (dashed line), native liquid control (solid line with X) and pressure-refolded after equilibration at 0.1 MPa (dotted line) are included on the plot for reference.

Figure 6: TEM micrographs of pressure-treated (A) thermally-induced aggregates, (B) guanidine hydrochloride-induced aggregates and (C) native control rhIFN-γ (no pressure treatment) at magnifications of 40,000. Short fibrous structures were observed in all samples, but the dominant structure was amorphous (*e.g.* A2). Bar = 200 μm.

Figure 7: Second derivative UV spectra of (A) thermally-induced and (B) guanidine hydrochloride-induced pressure-treated aggregates. All spectra were collected at 0.1 MPa immediately after completion of the pressure refolding protocol. Refolding was performed at 20 mg/mL (solid symbols), 10 mg/mL (open symbols) and 1 mg/mL (dotted line) and spectra collected immediately after dilution to *ca.* 1 mg/mL. The spectrum of rhIFN-γ native control (solid line) is superimposed in both windows for reference.

Figure 8: Area normalized second derivative FTIR spectra of pressure-treated (A) thermally-induced and (B) guanidine hydrochloride-induced aggregates. All spectra were collected at 0.1 MPa within three hours of the completion of the pressure refolding protocol. FTIR spectra were recorded for refolding performed at 20 mg/mL (solid symbols), 10 mg/mL (open symbols). The spectrum of rhIFN-γ native control (solid line) is superimposed in both windows for reference.

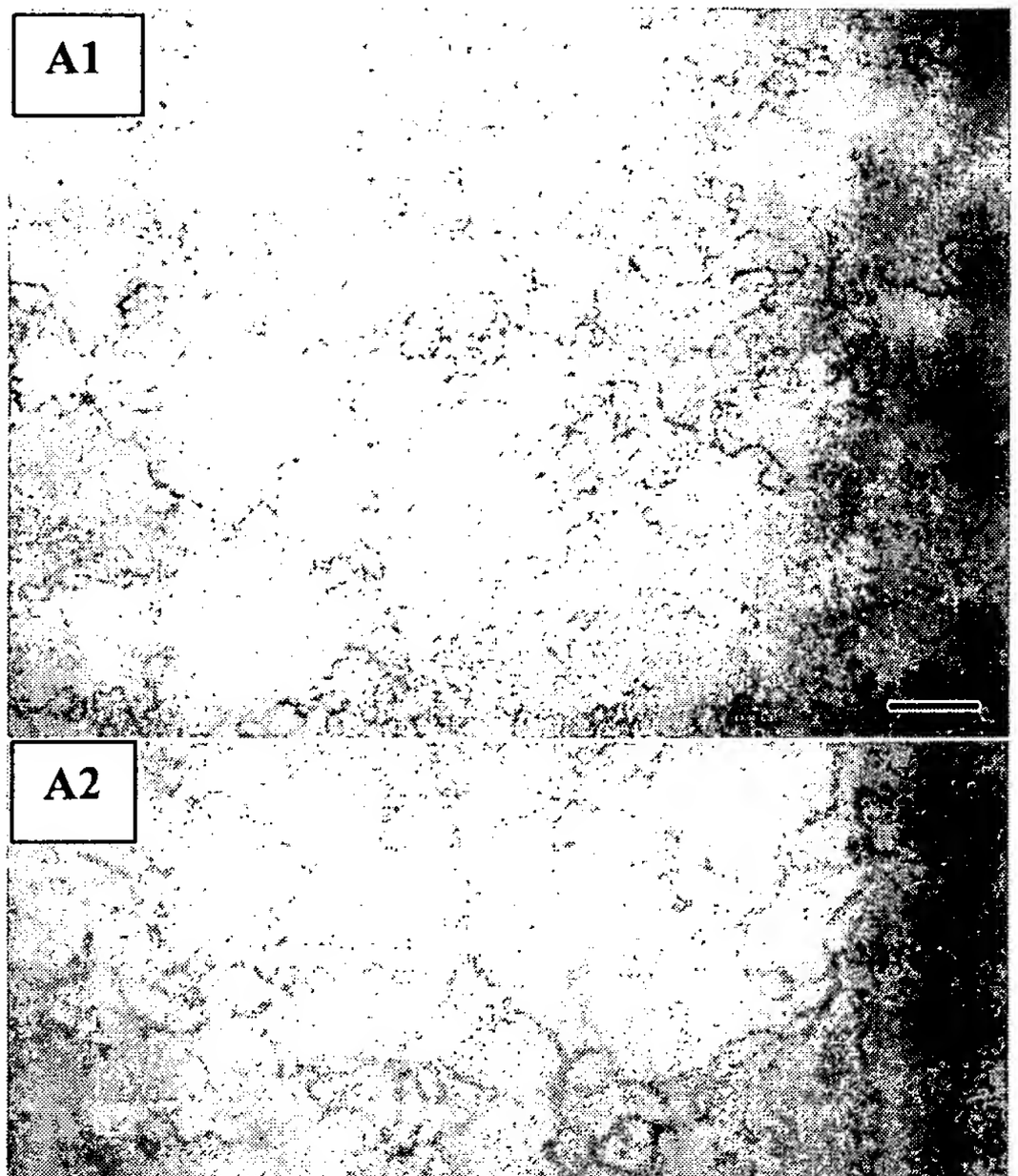

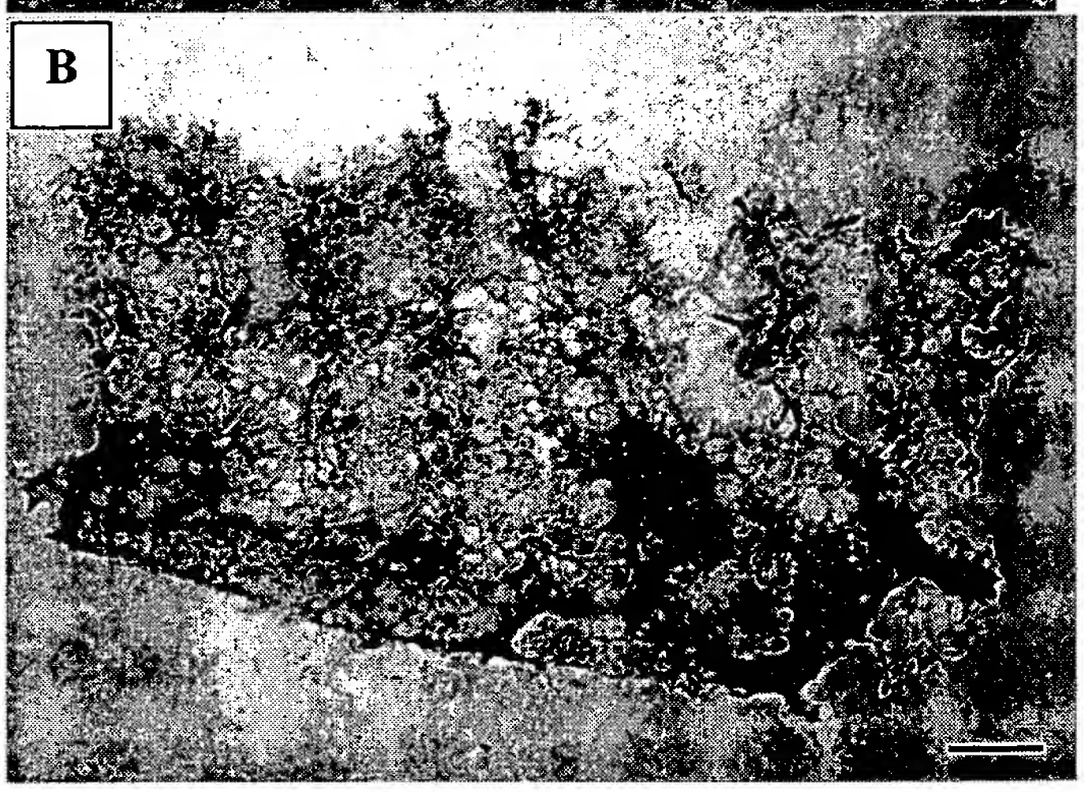

FIG. 1

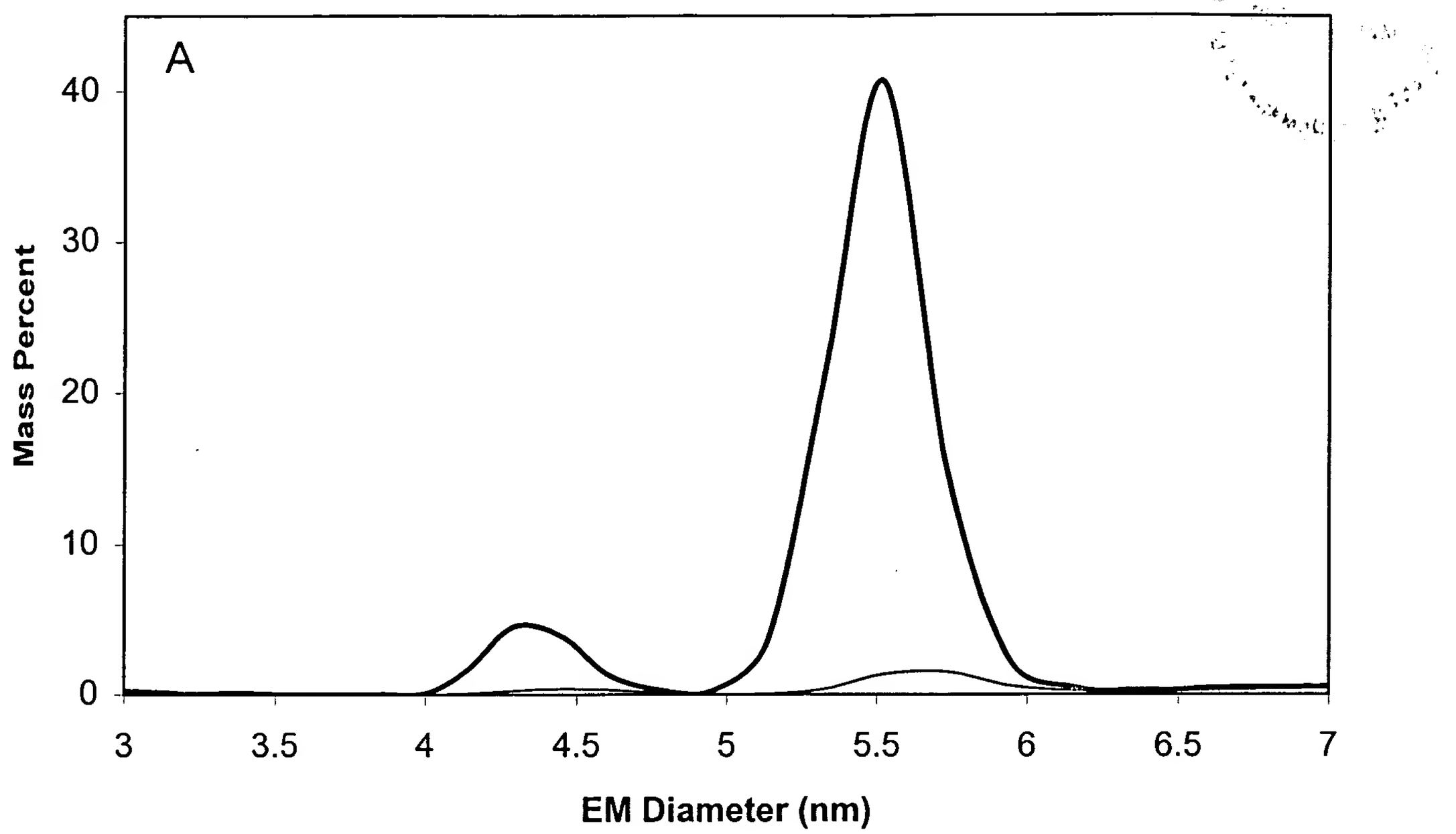
A
Mass Percent
40
30
20
10
0
3
3.5
4
4.5
5
5.5
6
6.5
7
EM Diameter (nm)

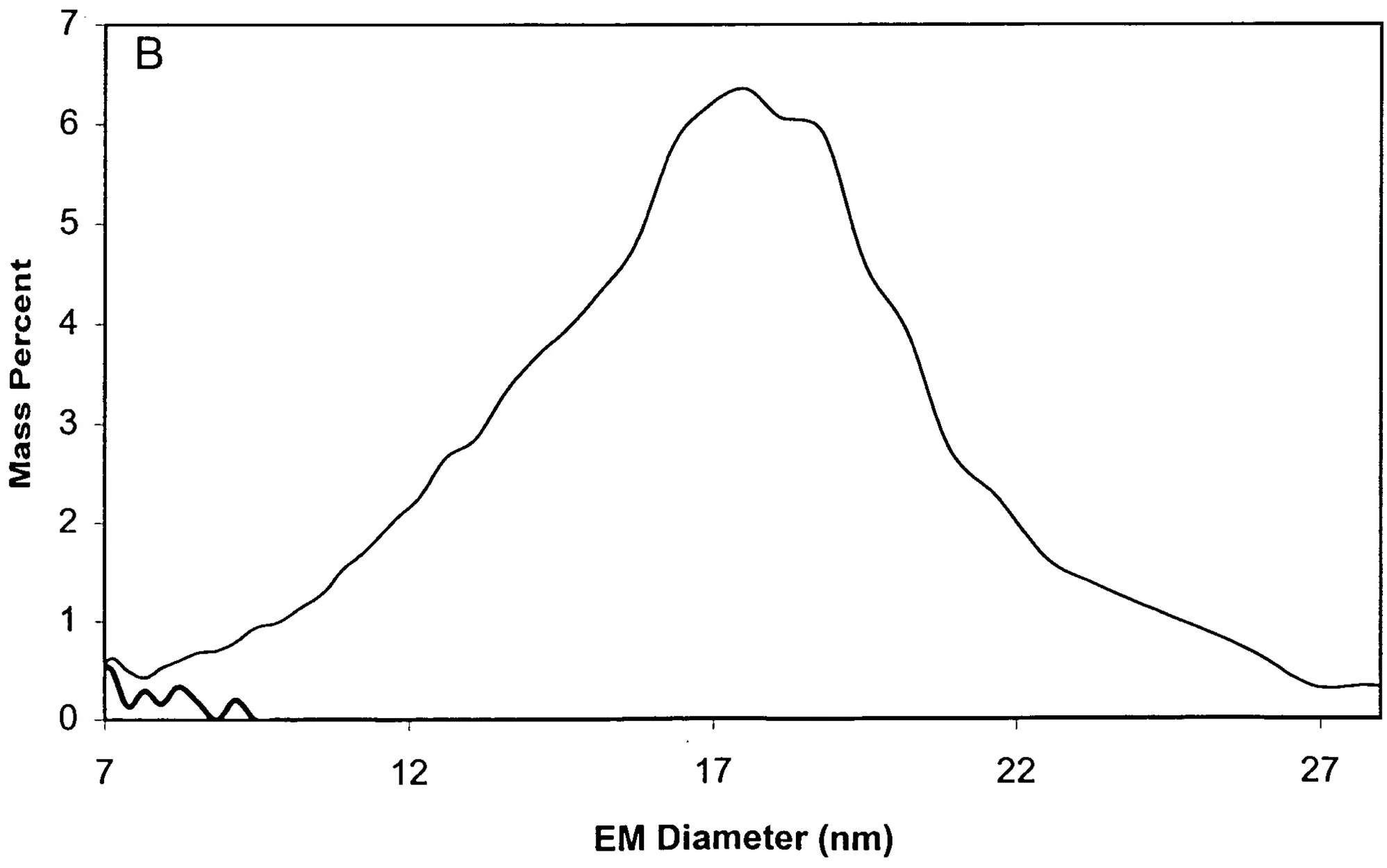
B
Mass Percent
7
6
5
4
3
2
1
0
7
12
17
22
27
EM Diameter (nm)

FIG. 2

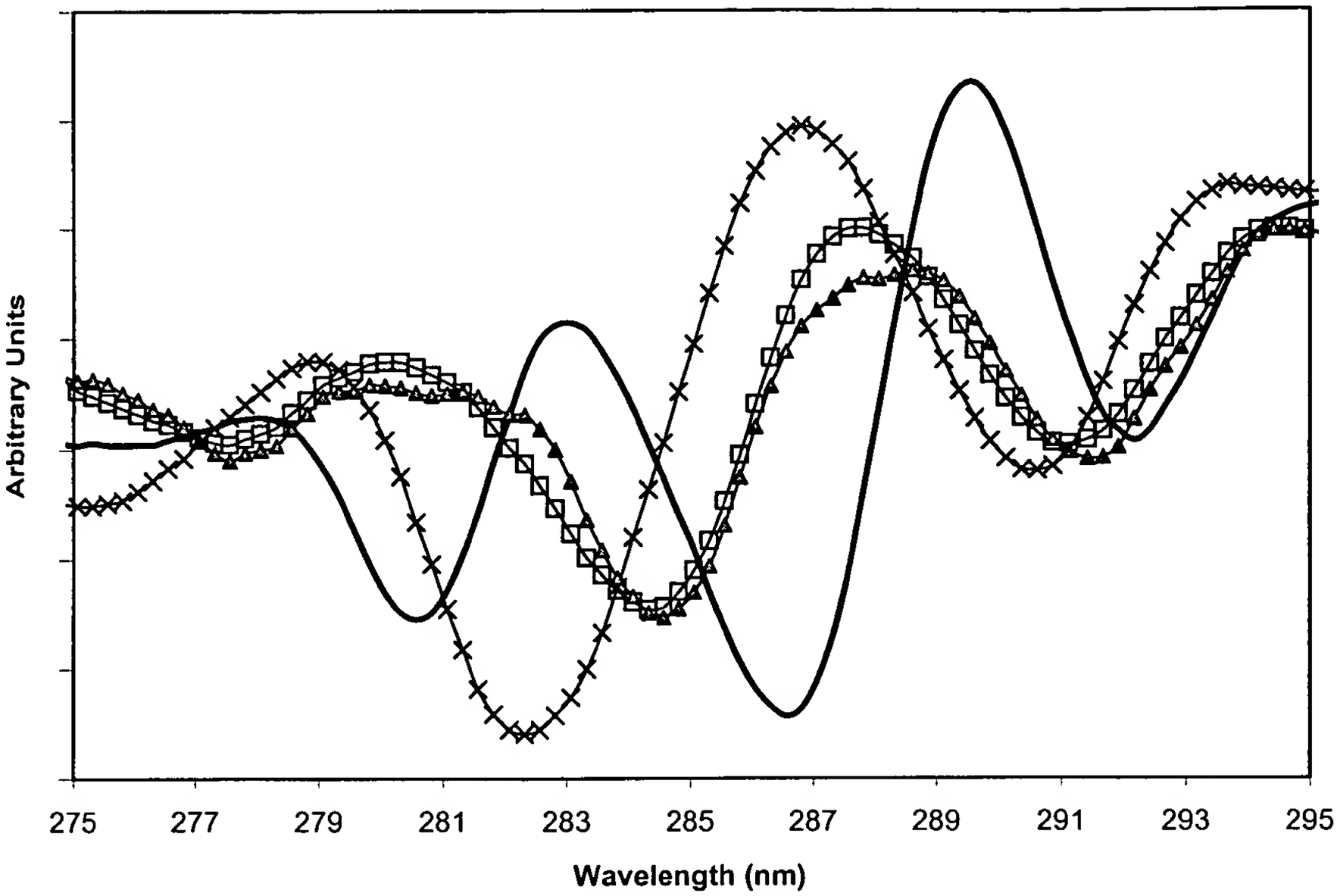
Arbitrary Units
275
277
279
281
283
285
287
289
291
293
295
Wavelength (nm)

FIG. 3

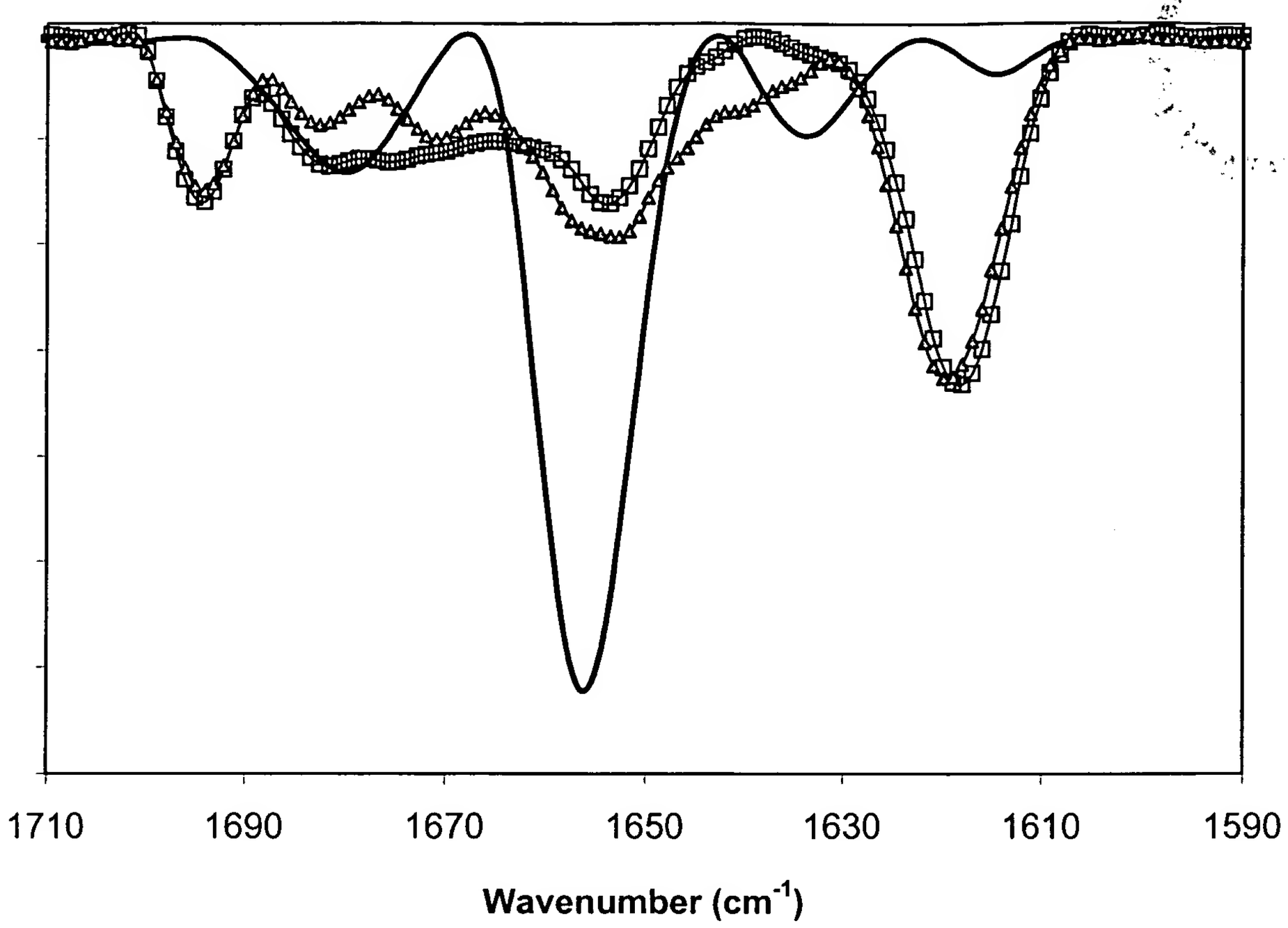
Arbitrary Units
1710
1690
1670
1650
1630
1610
1590
Wavenumber (cm-1)

FIG. 4

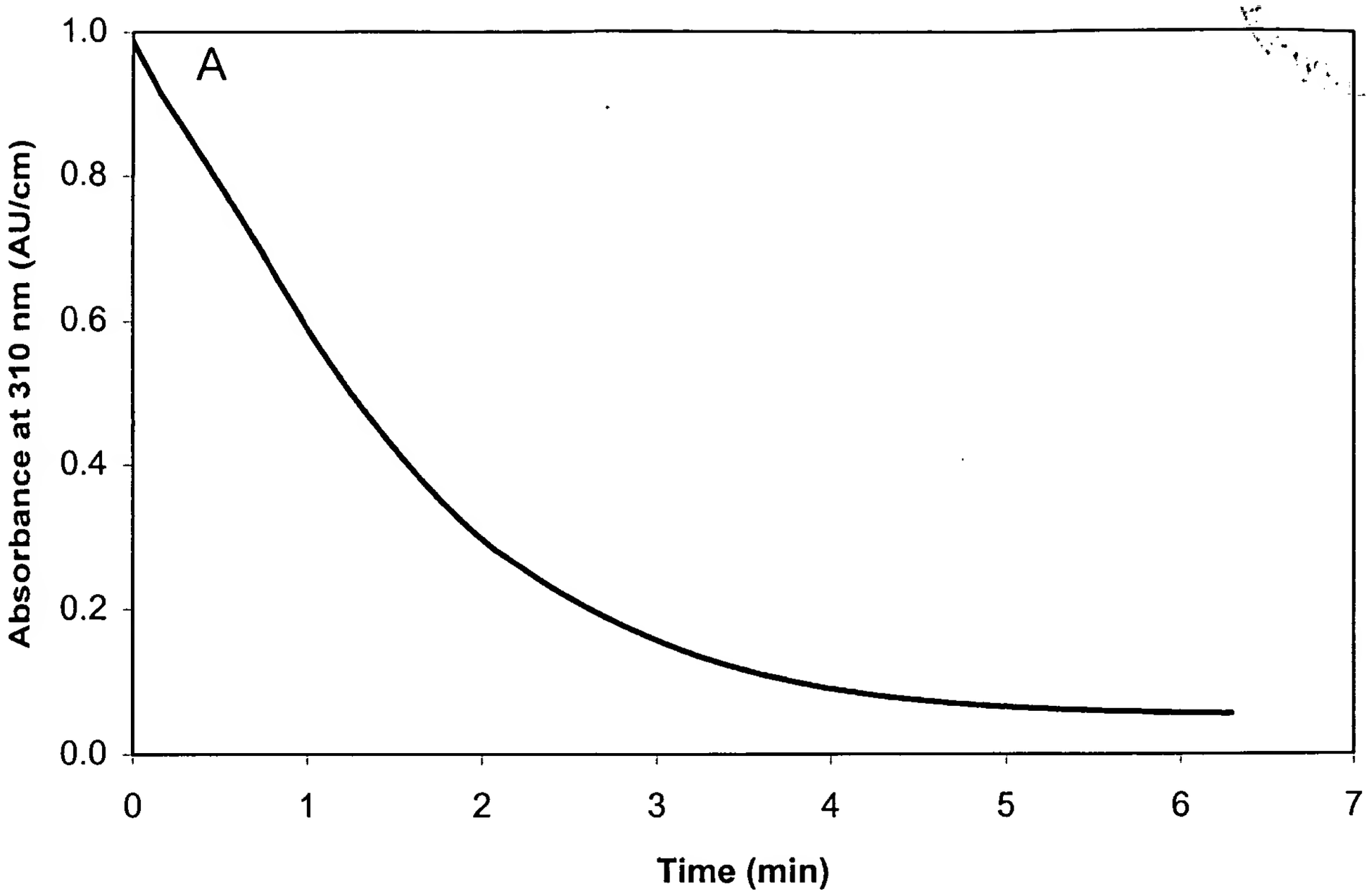
A
1.0
0.8
0.6
0.4
0.2
0.0
Absorbance at 310 nm (AU/cm)
0
1
2
3
4
5
6
7
Time (min)

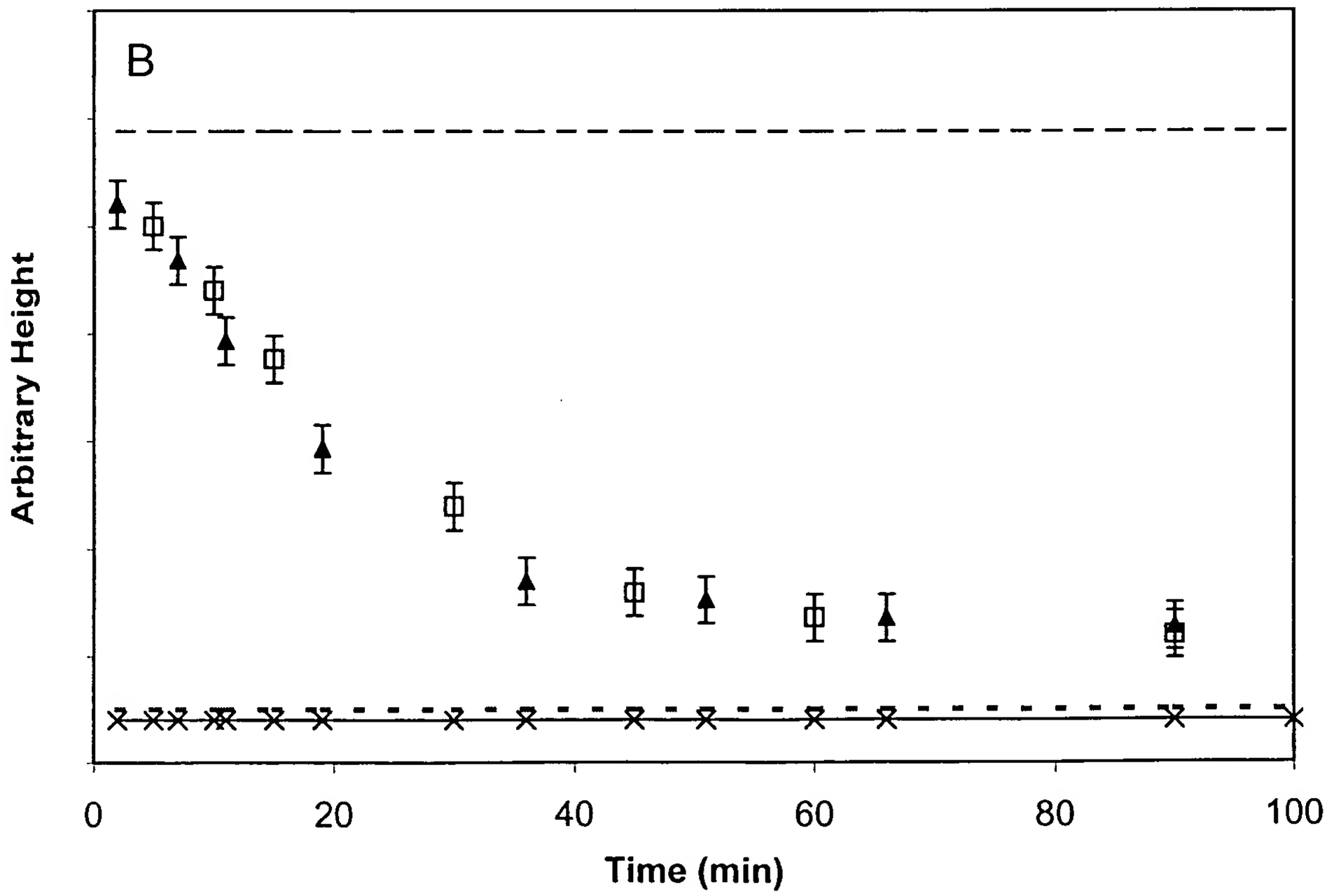
B
Arbitrary Height
0
20
40
60
80
100
Time (min)

FIG. 5

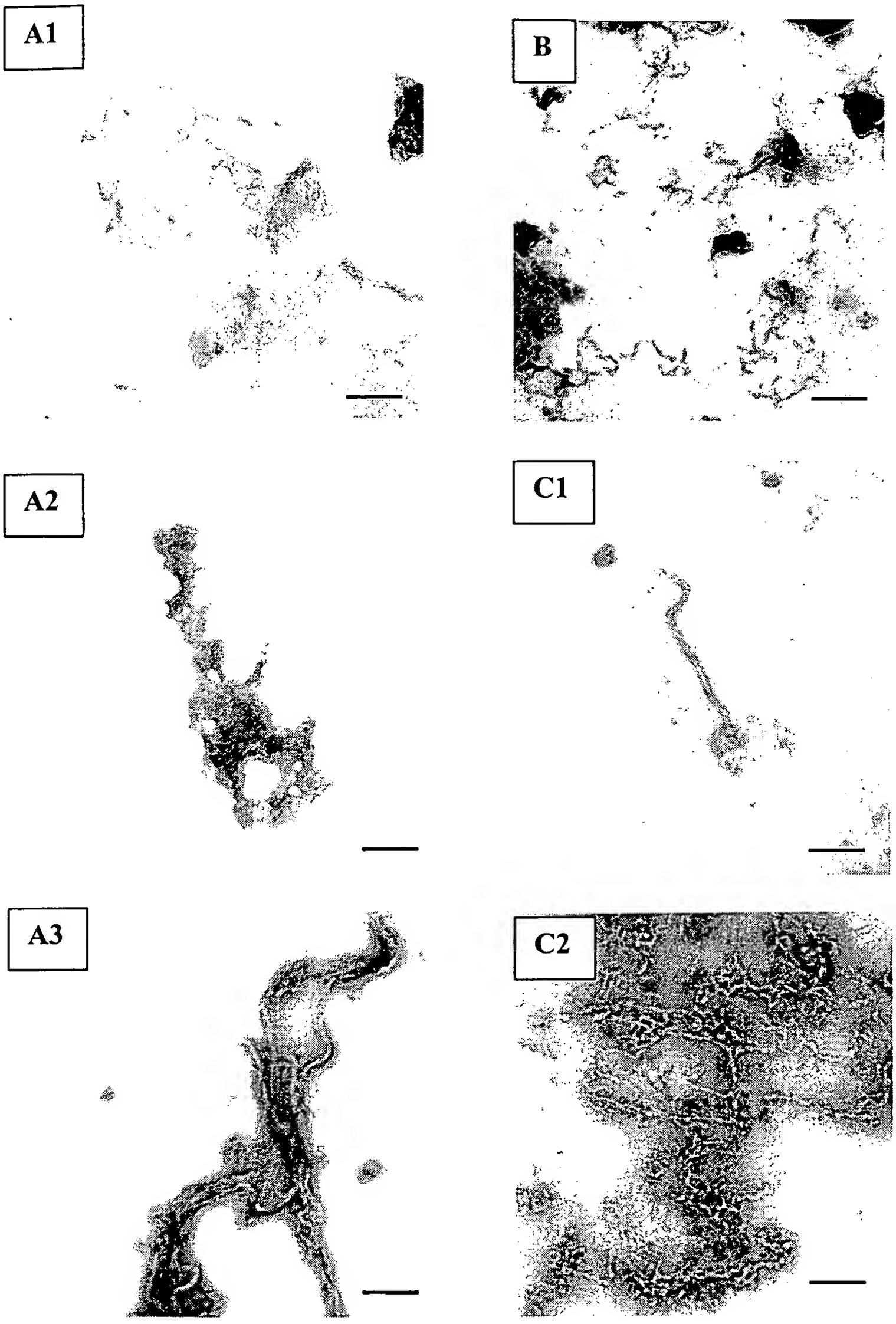

FIG. 6

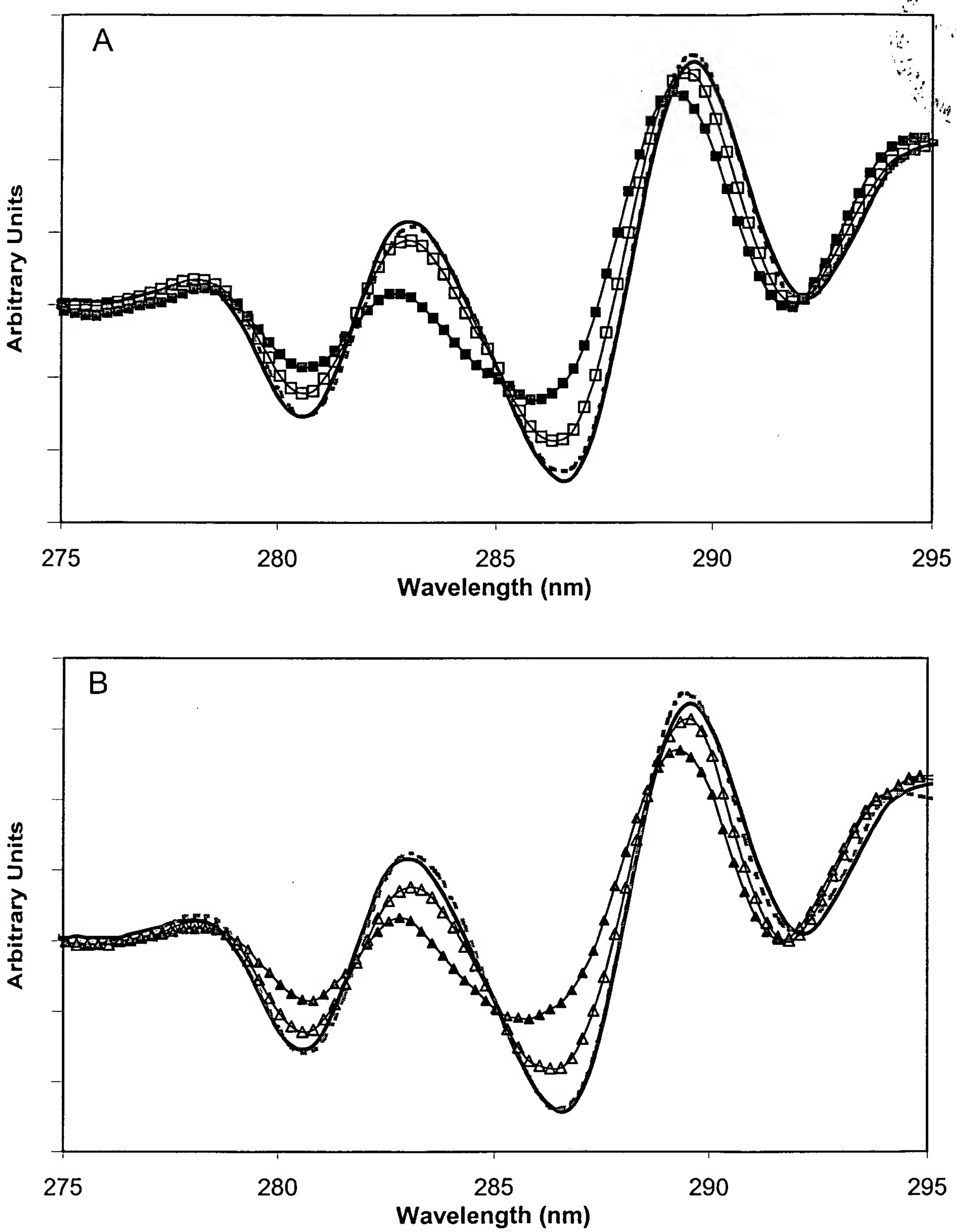
A
Arbitrary Units
275
280
285
290
295
Wavelength (nm)
B
Arbitrary Units
275
280
285
290
295
Wavelength (nm)

FIG. 7

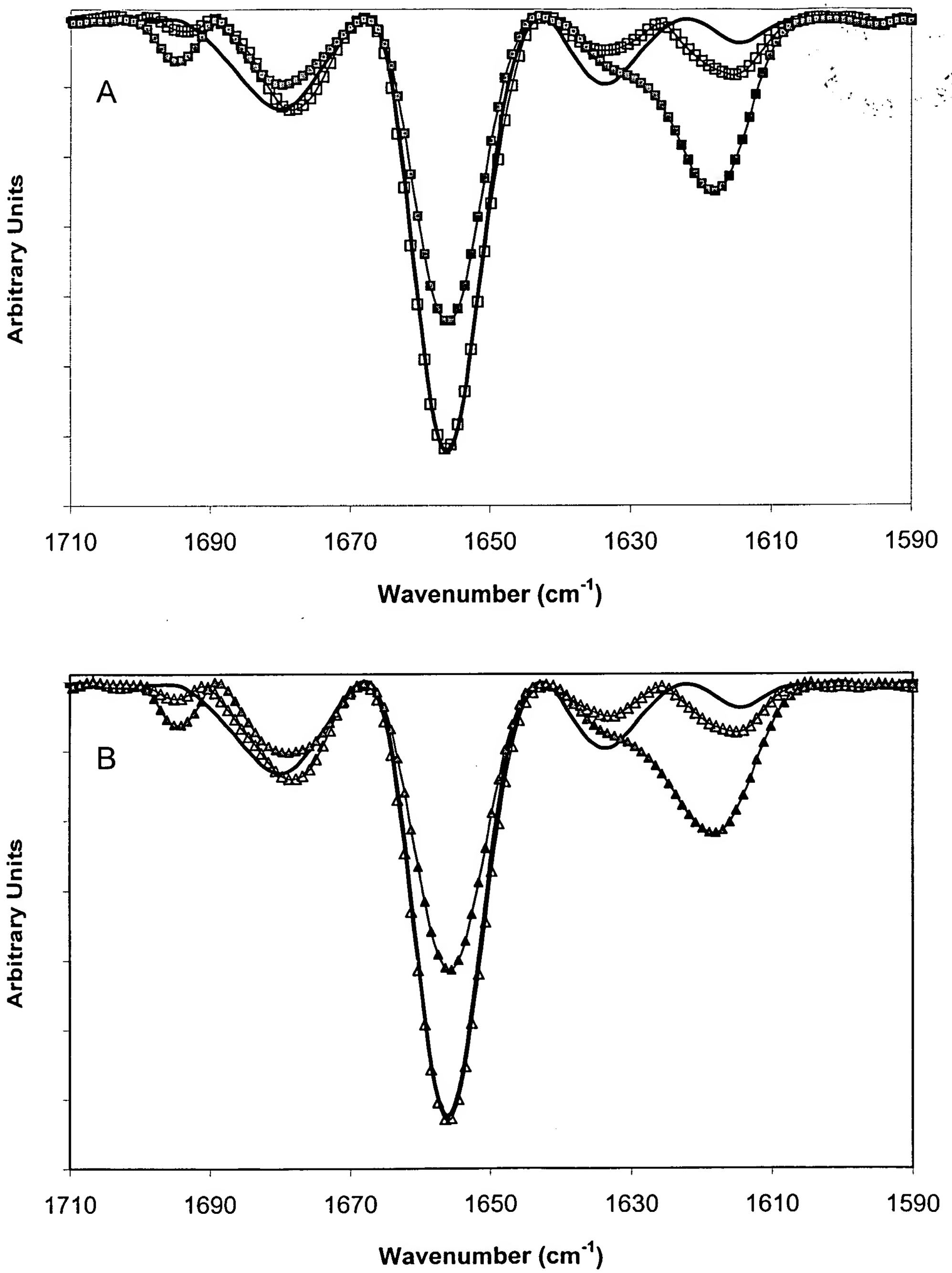
A
Arbitrary Units
1710
1690
1670
1650
1630
1610
1590
Wavenumber (cm-1)
B
Arbitrary Units
1710
1690
1670
1650
1630
1610
1590
Wavenumber (cm-1)

FIG. 8